NJC

Accepted Manuscript

This article can be cited before page numbers have been issued, to do this please use: J. Huang, B. Chen, B. Zhou and Y. Han, *New J. Chem.*, 2017, DOI: 10.1039/C7NJ03789A.

ROYAL SOCIETY OF CHEMISTRY

rsc.li/njc

DOI: 10.1039/C7NJ03789A

Journal Name

ARTICLE

A Novel ESIPT-Based Fluorescent Chemodosimeter for Hg^{2+} and Its Application in Live-Cell Imaging

Received 00th January 20xx,
Accepted 00th January 20xx

DOI: 10.1039/x0xx00000x

www.rsc.org/

Jing Huang, Bo Chen, Baocheng Zhou, and Yifeng Han*

A new excited-state intramolecular proton transfer (ESIPT) based fluorescent chemodosimeter for the detection of Hg^{2+} has been rationally designed and developed. The probe operates *via* the specific mercury-promoted desulfurization reaction of thiophthalimide to phthalimide and exhibits high selectivity and sensitivity in almost pure aqueous solution (containing only 1% DMSO) with a low detection limit of 1.5 ppb. Furthermore, the probe was successfully used for fluorescence imaging of Hg^{2+} in live cells.

Introduction

As one of the most ubiquitous and poisonous heavy metals, mercury has caused serious damage to the environment and human health.[1] Mercury is not biodegradable, and hence could be concentrated through the food chain in the tissues of fish and marine mammals.[2] Furthermore, mercury shows a strong affinity to sulfur-containing organic ligands, which causes the dysfunction of proteins and enzymes and results in a wide variety of diseases related to kidney, brain, and central nervous system damage.[3] Therefore, the determination of mercury in environmental and biological samples is crucial both to the monitoring of environmental pollution and to the diagnosis of clinical disorders.

Traditional analytical methods used for quantification of mercury species, such as inductively coupled plasma mass spectrometry,[4] atomic absorption-emission spectrometry,[5] anodic stripping voltammetry,[6] and reversed-phase high-performance liquid chromatography,[7] usually suffer from the expensive and sophisticated instrumentation, and/or complicated sample preparation, and are therefore not suitable for real-time and in situ analysis. While in contrast, small fluorescent probes usually display desirable sensitivity and selectivity, and are applicable to live cell detection due to their good cell membrane permeability and high spatial and temporal resolution, and therefore are getting more and more demanding in the bioanalytical field.[8]

Over the past several years, considerable efforts have been made to develop fluorescent probe for Hg^{2+} based on the coordination of Hg^{2+} to heteroatom-based ligands,[9] Hg^{2+} catalyzed devinylation reactions,[10] or Hg^{2+} catalyzed desulfurization reactions, including hydrolysis, cyclizations, and eliminations.[11] Although these reported probes are highly selective, many of them still have limitations such as low sensitivity, high detection limits, poor water solubility, long response time and laborious synthesis processes with expensive chemicals.[12] Therefore, the development of a simple yet highly sensitive, and water-soluble fluorescent probe for the detection of Hg^{2+} is still in high demand.

As a fragment of anticancer drug, Pomalidomide, 3-aminophthalimide has been reported as an important fluorophore exhibiting a large Stokes shift upon excitation by excited state intramolecular proton transfer (ESIPT) through the keto-enol tautomerism.[13] Furthermore, the fluorophore also possesses other favorable properties such as relatively high fluorescent quantum, good photostability, and facile preparation. In this work, we report a new fluorescent probe, **MS3** (mercury sensor) developed based on the 3-aminophthalimide skeleton for the detection of Hg^{2+} (Scheme 1). We envisioned that the fluorescent emission of the **MS3** would be greatly reduced due to the heavy atom effect of sulfur. However, desulfurization by mercury ions would promote the hydrolysis to releases the free phthalimide, which

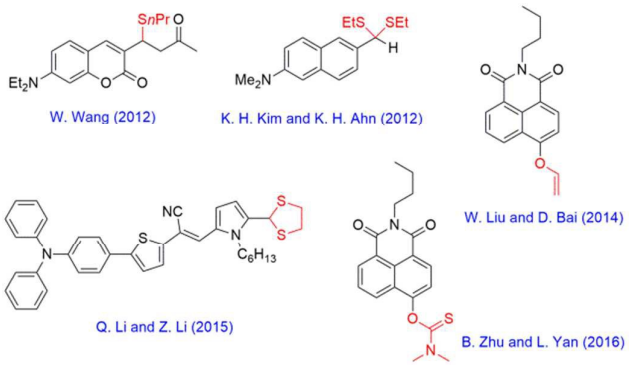

Fig. 1 Some reported mercury fluorescent probes.

Department of Chemistry, The Key Laboratory of Advanced Textile Materials and Manufacturing Technology, Zhejiang Sci-Tech University, Hangzhou, 310018, China.
E-mail: zstuchem@gmail.com; Tel: +86-751-86843550
Electronic Supplementary Information (ESI) available: Experimental details, characterization of the compounds, and additional spectroscopic data. See DOI: 10.1039/x0xx00000x

View Article Online
DOI: 10.1039/C7NJ03789A

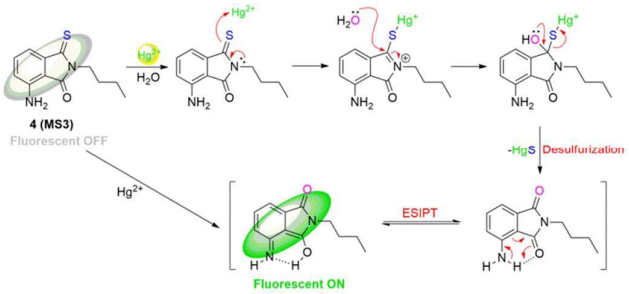

Scheme 1 Fluorescent turn-on sensing of Hg^{2+} by **MS3**.

wills recover its highly fluorescent emission (Scheme 1). To the best of our knowledge, this is the first example of an ESIPT-based fluorescent chemodosimeter using Hg^{2+}-mediated desulfurization of thioimide for the selective mercury ions detection. Furthermore, **MS3** can be successfully applied to image Hg^{2+} in live cells.

Experimental section

General methods

All the solvents were of analytic grade. NMR experiments were carried out on a Bruker AV-400 NMR spectrometer with chemical shifts reported in ppm (in $CDCl_3$, d_6-DMSO, or TMS as an internal standard). Mass spectra were measured on an Agilent 1290 LC-MS spectrometer. All pH measurements were made with a Sartorius basic pH-Meter PB-10. Fluorescence spectra were determined on a PerkinElmer LS55 Fluorescence spectrophotometer. Absorption spectra were collected on a Shimadzu UV 2501(PC)S UV-Visible spectrophotometer. All the cation solutions were prepared from NaCl, KCl, $CaCl_2$, $MgCl_2$, $MnCl_2$, $ZnCl_2$, $CoCl_2$, $CrCl_2$, $CuCl_2$, $FeCl_2$, $FeCl_3$, $NiCl_2$, $Pb(OAc)_2$, $SnCl_4$, $AgNO_3$, and $Hg(ClO_4)_2$ in distilled water, with a concentration of 1 mM, respectively. The excitation and emission widths for **MS3** were all 3/3.

Synthesis

N-butyl-3-nitrophthalimide (2): was synthesized according to the literature.[13a] ^{1}H NMR (400 MHz, Chloroform-*d*) δ 8.11 (m, 2H), 7.91 (dd, *J* = 8.0, 7.2 Hz, 1H), 3.73 (t, *J* = 7.3 Hz, 2H), 1.68 (m, 2H), 1.40 (m, 2H), 0.95 (t, *J* = 7.2 Hz, 3H).

N-butyl-3-aminophthalimide (3): The mixture of compound **2** (1.50 g, 6.04 mmol) and Pd/C 10% (200 mg) in methanol (50 mL) was stirred under hydrogen atmosphere (hydrogen balloon) at room temperature for 12 h. The catalyst was filtered off and rinsed with methanol. The filtrate was concentrated, and the residue was dried under vacuum for 1 h to give **3** (1.26 g, 96%) as a light yellow solid. ^{1}H NMR (400 MHz, Chloroform-*d*) δ 7.33 (dd, *J* = 8.4, 7.2, 1H), 7.07 (d, *J* = 6.8 Hz, 1H), 6.82 (d, *J* = 8.4 Hz, 1H), 5.32 (brs, 2H), 3.58 (t, *J* = 7.2 Hz, 2H), 1.59 (q, *J* = 7.4 Hz, 2H), 1.32 (q, *J* = 7.5 Hz, 2H), 0.90 (t, *J* = 7.4 Hz, 3H). ^{13}C NMR (100 MHz, Chloroform-*d*) δ 170.18, 168.62, 145.11, 134.91, 132.65, 121.14, 112.45, 111.07, 37.18, 30.58, 19.92, 13.64.

7-amino-2-butyl-3-thioxoisoindolin-1-one (4, MS3): The mixture of compound **3** (500 mg, 2.29 mmol) and Lawesson's reagent (1.02 g, 2.52 mmol) in dry PhMe (10 mL) was refluxed under nitrogen atmosphere for 4 h until all starting material got consumed which was monitored by TLC analysis. The solvent was removed under vacuum and the product was purified by flash chromatography using petroleum ether/EtOAc (5:1, v/v) as eluant to give **4** (0.37 g, 65%) as a red solid. ^{1}H NMR (400 MHz, Chloroform-*d*) δ 7.34 (t, *J* = 7.6 Hz, 1H), 7.25 (d, *J* = 7.3 Hz, 1H), 6.82 (d, *J* = 8.3 Hz, 1H), 5.20 (brs, 2H), 3.95 (t, *J* = 7.3 Hz, 2H), 1.67 (q, *J* = 7.4 Hz, 2H), 1.36 (q, *J* = 7.5 Hz, 2H), 0.92 (t, *J* = 7.3 Hz, 3H). ^{13}C NMR (100 MHz, Chloroform-*d*) δ 196.83, 171.31, 144.59, 138.04, 135.07, 120.32, 113.57, 40.42, 30.00, 20.13, 13.70. HR-MS (TOF-ESI): Calcd. for $([M])^+$, 235.0905; Found, 235.0897.

Cell culture and imaging

HeLa cells were cultured in DMEM (Invitrogen, Carlsbad, CA), supplemented with 10% fetal bovine serum in a humidified atmosphere of 5% CO_2 at 37 °C. For imaging experiments, **e**xponentially growing cells were seeded in 24-well plate. Cells were cultured at 37 °C in a 5% CO_2 atmosphere for 24 h before they were exposed to reagents.

For labeling, the medium was removed and cells were rinsed three times with PBS. Then HeLa cells were incubated with **MS3** (10 μM) in PBS (containing 1% EtOH) at 37 °C for 30 min as control. For Hg^{2+} imaging, another set of HeLa cells was preloaded with **MS3** (10 μM) in PBS (containing 1% EtOH) at 37 °C for 30 min, rinsed three times with PBS and further treated with different concentrations of Hg^{2+} (10, 15, and 20 μM, respectively) in PBS at 37 °C for additional 30 min. Cells were rinsed three times with PBS and bathed in it, then imaging was carried out. Images were acquired using an inverted fluorescence microscope and fluorescence imaging was performed in a blue channel.

Results and discussion

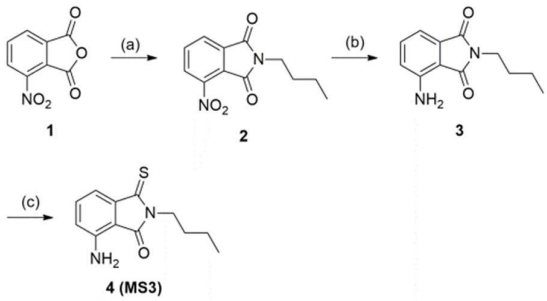

Scheme 2 Synthesis of **MS3**: (a) *n*-butylamine, AcOH, reflux, 2 h, 83%; (b) Pd/C, H_2, MeOH, r.t., 12 h, 96%; (c) Lawesson's Reagent, PhMe, reflux, 4 h, 69%.

As shown in Scheme 2, **MS3** can be readily prepared in three steps under facile conditions with good yields starting with commercially available 3-nitrophthalic anhydride. The product

DOI: 10.1039/C7NJ03789A

(**MS3**) was well characterized by ^{1}H, ^{13}C NMR, HMBC, and HR-MS (ESI†).

UV-vis and fluorescence spectral responses of MS3 to Hg^{2+}

With **MS3** in hand, we firstly assessed the UV-vis spectroscopic properties of **MS3** in PBS buffer solution (10 mM, pH 7.4, containing 1% DMSO) (Fig. 2 and S1-2, ESI†). **MS3** (20.0 μM) displayed a moderate UV-vis absorption around 438 nm. Upon incremental addition of Hg^{2+} (0-5.0 equiv.), the peak at 438 nm dramatically decreased, and a new band at 386 nm, which is characteristic for the 3-aminophthalimide fluorophore (Fig. S3, ESI†),[13a] appeared instantly with four clear isosbestic points at 295, 321, 416, and 513 nm, respectively, (blue-shift about 52 nm with a marked color change from light yellow to colorless), indicating that compound **3** (3-aminophthalimide) was formed in the present of Hg^{2+}. Furthermore, a good linear relationship (R^2 = 0.9967) was observed between the changes in the ratios of absorbance at 386 and 438 nm (A_{386} nm/A_{438} nm) with Hg^{2+} in the range of 0-5.0 equiv. (Fig. 2 and S1, ESI†).

The emission spectra of **MS3** and its fluorescent titration with Hg^{2+} were also recorded in PBS buffer solution (10 mM, pH 7.4, containing 1% DMSO) (Fig. 3 and S4, ESI†). As expected, **MS3** alone is almost non-fluorescent (λ_{ex} = 392 nm, λ_{em} = 501 nm, Φ = 0.01, Table S1, ESI†) due to the increasement of the intersystem crossing (ISC) rate affected by the heavy-atom (sulfur).[14] However, upon progressive addition of Hg^{2+} (0-35.0 equiv.), an emission band centered at 501 nm rapidly increased, which was deduced to be attributed to the formation of the free ESIPT active 3-aminophthalimide fluorophore by the Hg^{2+}-mediated desulfurization of the thiophthalimide group in **MS3** (Stokes-shift of 109 nm with a marked color change from dark to green) (Fig. 3 and Scheme 1). Moreover, the fluorescence titration curve revealed that the fluorescence intensity of **MS3** at 501 nm increased linearly with increasing concentrations of Hg^{2+} (Fig. 3, and S4, ESI†) and further smoothly increased until a maximum was reached up to 15.0 equiv. of Hg^{2+} (Φ = 0.49, Table S1). Owing to the specific reactivity of mercury ion-promoted hydrolysis reaction, **MS3** displayed a high sensitivity toward Hg^{2+} (about 116-fold fluorescent enhancement). For practical purposes, the detection limit of **MS3** for the analysis of Hg^{2+} was also an important parameter. The fluorescence titration curve revealed that the fluorescence intensity of **MS3** at 501 nm increased linearly with the amount of Hg^{2+} in the range of 0-2.5 μM (R^2 = 0.99) (Fig. S5, ESI). Thus, the detection limit of **MS3** for Hg^{2+} was calculated to be 7.48×10^{-9} M (Hg^{2+} content = 1.5 ppb), which was below the USA Environmental Protection Agency (EPA) threshold in safe drinking water (2.0 ppb).[15] These results showed that **MS3** could be a sensitive fluorescent probe for the quantitative detection of Hg^{2+}.

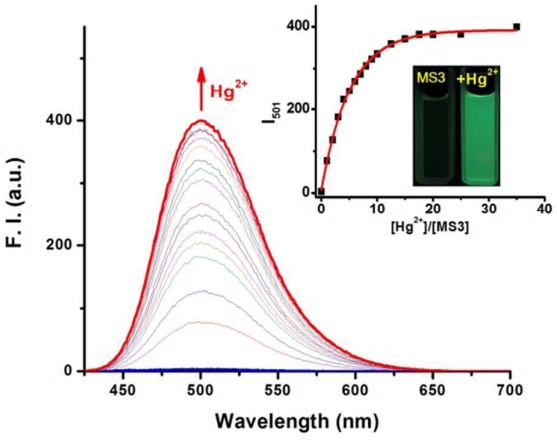

Fig. 3 Fluorescence spectra of **MS3** (10.0 μM) in PBS buffer solution (10 mM, pH 7.4, containing 1% DMSO) in the presence of different concentrations of Hg^{2+} (0-35.0 equiv.). (λ_{ex} = 392 nm). Inset 1: the fluorescent intensity of **MS3** at 501 nm as a function of Hg^{2+} concentration (0-35.0 equiv.). Inset 2: cuvette images of probe **MS3** before and after addition of Hg^{2+} taken under a hand-held UV-lamp (λ_{ex} = 365 nm).

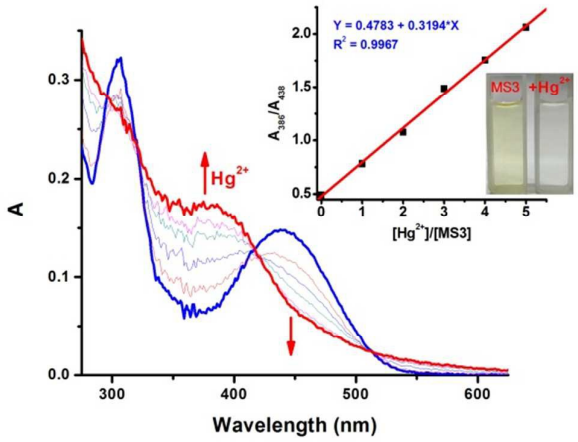

Fig. 2 Absorption spectra of **MS3** (20.0 μM) in PBS buffer solution (10 mM, pH 7.4, containing 1% DMSO) in the presence of different concentrations of Hg^{2+} (0-5.0 equiv.). Inset 1: the ratio of the UV-vis absorption of **MS3** (20.0 μM) at 386 nm and 438 nm as a function of Hg^{2+} concentration. Inset 2: cuvette images of probe **MS3** before and after addition of Hg^{2+}.

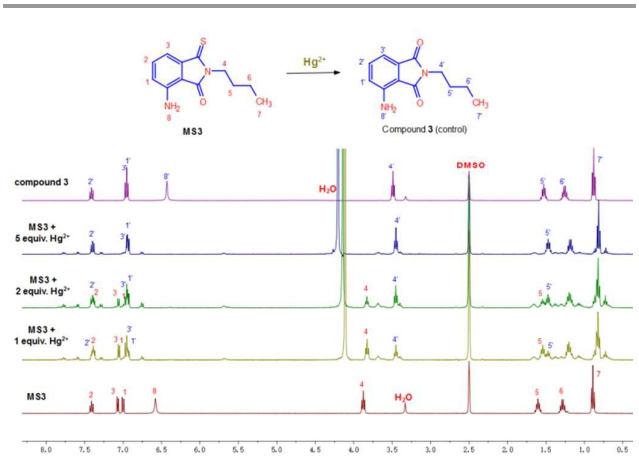

Fig. 4 ^{1}H NMR titration experiment of **MS3** in the presence of different concentrations of Hg^{2+} (0-5.0 equiv. of Hg^{2+}, in d_6-DMSO).

View Article Online
DOI: 10.1039/C7NJ03789A

^{1}H NMR titration experiments of MS3

Efforts were then made to check the detecting mechanism as envisioned that the Hg^{2+}-induced desulfurization of the thiophthalimide of **MS3** to the free ESIPT active 3-aminophthalimide (Scheme 1). To this end, a comparison of IR spectra between the **MS3** and **MS3**–Hg^{2+} system was made to confirm the desulfurization of **MS3** after treatment with Hg^{2+} (Fig. S6, ESI†). The HR-MS spectra of the isolated product of the **MS3**–Hg^{2+} solution were also measured to support the generation of 3-aminophthalimide by Hg^{2+} (Fig. S7, ESI†). Furthermore, ^{1}H NMR titration experiment was also conducted. As shown in Fig. 4, the two aromatic protons at δ 7.07 (1H, d, J = 6.8 Hz) and 7.00 (1H, d, J = 8.8 Hz) attributed to the H-3 and H-1, respectively, disappeared gradually after the increasement addition of Hg^{2+}. Meanwhile, chemical shifts of protons at δ 6.95 (1H, d, J = 6.8 Hz), 6.93 (1H, d, J = 8.4 Hz), attributed to the H-3', H-1', respectively, were discovered, indicating that the hydrolytic desulfurization of thiophthalimide group of **MS3** occurred in the presence of Hg^{2+} (Scheme 1). Furthermore, the aliphatic protons at δ 3.88 (2H, t, J = 7.2 Hz) and 1.61 (2H, q, J = 7.2 Hz) attributed to the H-5 and H-6, respectively, were dramatically shifted upfield to 3.45 (2H, t, J = 7.2 Hz, H-5') and 1.47 (2H, q, J = 7.2 Hz, H-6'), respectively, after the addition of Hg^{2+} due to the desulfurization process strengthens the electron-donating ability from nitrogen atom. Those results are in agreement with the optical response.

Time-dependent experiment of MS3

Subsequently, the time-dependence of fluorescence was also evaluated in the presence of different concentration of Hg^{2+} in PBS buffer solution (10 mM, pH 7.4, containing 1% DMSO) (Fig. 5 and S8-12, ESI†). The result shows that the fluorescence of tested solutions (eg: in the presence of 10, 15, and 20 equiv. of Hg^{2+}) remarkably increased to their maximum value within the 5 minutes. And no changes in fluorescence were detected in the absence of Hg^{2+} (Fig. 5 and S8-12, ESI†). Furthermore, the pseudo-first-order rate constant of **MS3** is calculated to be k = 0.612 min^{-1} for Hg^{2+} in PBS buffer solution (10 mM, pH 7.4, containing 1% DMSO) (Fig. S13, ESI).

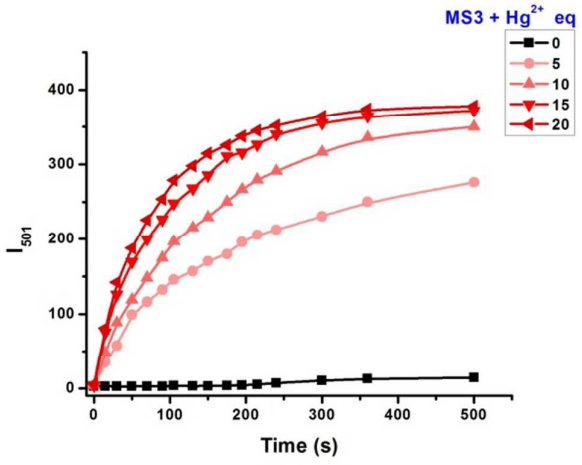

Fig. 5 Time-dependent fluorescence intensity changes of **MS3** (10.0 μM) upon addition of various concentration of Hg^{2+} (0, 5, 10, 15, and 20 equiv. each) in PBS buffer solution (10 mM, pH 7.4, containing 1% DMSO) (λ_{ex} = 392 nm).

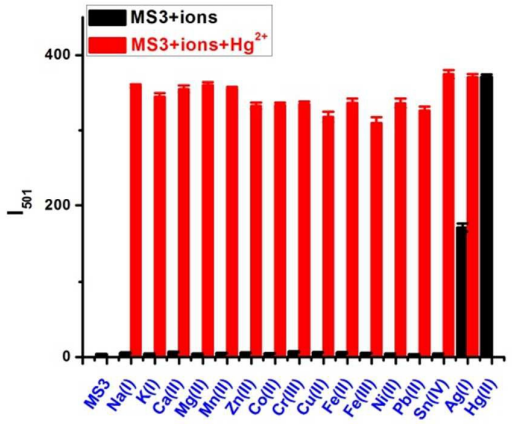

Fig. 6 Fluorescence responses of **MS3** to various metal ions (including Na^+, K^+, Ca^{2+}, Mg^{2+}, Mn^{2+}, Zn^{2+}, Co^{2+}, Cr^{3+}, Cu^{2+}, Fe^{2+}, Fe^{3+}, Ni^{2+}, Pb^{2+}, Sn^{4+}, Ag^+, and Hg^{2+}). Black bars represent the addition of 15.0 equiv. of the appropriate metal ions to a 10.0 μM solution of **MS3** (in PBS buffer solution, 10 mM, pH 7.4, containing 1% DMSO). Red bars represent the addition of 15.0 equiv. of Hg^{2+} to the solutions containing **MS3** (10.0 μM) and the appropriated metal ions (15.0 equiv.) (λ_{ex} = 392 nm).

The selection and competition experiments of MS3

Continuing on, the fluorescence titration of **MS3** with various metal ions was conducted to examine the selectivity (Fig. 6 and Fig. S14, ESI†). Much to our delight, the turn-on response of **MS3** is highly specific for Hg^{2+} and no obvious change of fluorescent emission was observed when it is treated with Na^+, K^+, Ca^{2+}, Mg^{2+}, Mn^{2+}, Zn^{2+}, Co^{2+}, Cr^{3+}, Cu^{2+}, Fe^{2+}, Fe^{3+}, Ni^{2+}, Pb^{2+}, and Sn^{4+}. It should be mentioned that as most of the existing Hg^{2+}-fluorescent probe, Ag^+ ions also has a slight fluorescent response to **MS3** (Fig. 6 and Fig. S14, ESI†). However, the addition of NaCl to the tested buffer solution (PBS buffer solution, 10 mM, pH 7.4, containing 1% DMSO) is the simple but useful method to distinguish Hg^{2+} from Ag^+ because of the high binding affinity between Ag^+ and Cl^- (AgCl, K_{sp} = 1.8 × 10^{-10}).

Moreover, in the following competing experiments (Fig. 6 and Fig. S15, ESI†), no significant response in the fluorescence intensity was found by comparison with that without the other metal ions besides Hg^{2+}, which implies that **MS3** bears high selectivity for Hg^{2+} in the presence of other competitive metal ions.

pH titration of MS3

Moreover, the Hg^{2+}-sensing ability of **MS3** at a wide range of pH values was investigated. As depicted in Fig. S16 and S17,

View Article Online
DOI: 10.1039/C7NJ03789A

ESI,† **MS3** alone was inert to pH in the range of 4.5-9.0. But in the presence of Hg^{2+}, the fluorescence response scope of **MS3** decreased when the surrounding pH decreased (Fig. S16 and S18, ESI†), which was due to the fact that sulfur atom could be protonated in acidic conditions and lost its nucleophilicity. These results are also consistent with the proposed mechanism (Scheme 1). However, satisfactory Hg^{2+}-sensing abilities were exhibited in the range of pH from 6.0 to 9.0, indicating that **MS3** could be used in living cells without interference from pH effects.

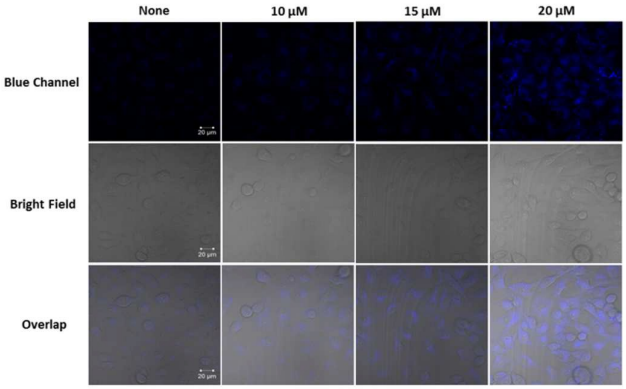

Fig. 7 Fluorescence images of HeLa cells with **MS3** (10.0 μM) and different concentration of Hg^{2+} (0, 10.0, 15.0, and 20.0 μM, respectively) for 30 min.

Cell imaging

Due to the favorable properties of **MS3** in vitro, its potential application in living cells was studied. For this purpose, HeLa cells were first incubated with **MS3** (10.0 μM) for 30 min, then Hg^{2+} (0, 10.0, 15.0, and 20.0 μM, respectively) was added and incubated for another 30 min at 37 ^{o}C, and the fluorescence images were taken. As shown in Fig. 7, cells without the treatment of Hg^{2+} showed weak blue fluorescence, whereas the cells exposed to both **MS3** and Hg^{2+} displayed strong blue fluorescence and the intracellular fluorescence intensities correlated with the concentration of Hg^{2+} added (from 10 to 20 μM) (Fig. 7). These obvious changes indicated that **MS3** was a cell membrane permeable and capable of imaging Hg^{2+} in living cells. Furthermore, the series of bright field images shown that the cells were intact, healthily spread and adherent during and after the labeling process with **MS3** indicating that the probe has no cytotoxic effect, which has also been further confirmed by MTT assay (Fig. S20, ESI).

Conclusions

In conclusion, we have rationally developed a new and simple ESIPT-based sensitive fluorescent probe for the selective detection of Hg^{2+} *via* mercury-triggered desulfurization reaction. The probe has the unique advantage of easy-preparation, good water solubility, low detection limit, and fast and specific response towards Hg^{2+} under mild conditions. Furthermore, fluorescence imaging of Hg^{2+} in live cells indicated that this probe might be favorable for biological applications.

Acknowledgements

This work was supported by Zhejiang Provincial Natural Science Foundation of China (Grant No. LY17B070008), Zhejiang Province Public Welfare Projects (Grant No.2016C37046), and the Project Grants 521 Talents Cultivation of Zhejiang Sci-Tech University.

Notes and references

1 M. F. Wolfe, S. Schwarzbach and R. A. Sulaiman, *Environ. Toxicol. Chem*., 1998, **17**, 146.
2 P. Grandjean, P. Weihe, R. F. White and F. Debes, *Environ. Res*., 1998, **77**, 165.
3 (*a*) C. R. Baum, *Curr. Opin. Pediatr*., 1999, **11**, 265; (*b*) R. K. Zalups and S. Ahmad, *J. Am. Soc. Nephrol*., 2004, **15**, 2023.
4 B. Fong, W. Mei, T. S. Siu, J. Lee, K. Sai and S. Tam, *J. Anal. Toxicol*., 2007, **31**, 281.
5 A. Bernaus, X. Gaona, J. M. Esbrı, P. Higueras, G. Falkenberg and M. Valiente, *Environ. Sci. Technol*., 2006, **40**, 4090.
6 O. Abollino, A. Giacomino, M. Malandrino, G. Piscionieri and E. Mentasti, *Electroanalysis*, 2008, **20**, 75.
7 L. Wang, J. B. Zhou, X. Wang, Z. H. Wang and R. S. Zhao, *Anal. Bioanal. Chem*., 2016, **408**, 4445.
8 (*a*) J. Li, D. Yim, W.-D. Jang and J. Yoon, *Chem. Soc. Rev*., 2017, **46**, 2437; (*b*) M. Gao, F. Yu, C. Lv, J. Choo and L. Chen, *Chem. Soc. Rev*., 2017, **46**, 2237; (*c*) X. Chen, F. Wang, J. Y. Hyun, T. Wei, J. Qiang, X. Ren, I. Shin and J. Yoon, *Chem. Soc. Rev*., 2016, **45**, 2976; (*d*) X. Sun, Y. Wang and Y. Lei, *Chem. Soc. Rev*., 2015, **44**, 8019; (*e*) J. Liu, W. Bu and J. Shi, *Chem. Rev*., 2017, **117**, 6160; (*f*) J. Zielonka, J. Joseph, A. Sikora, M. Hardy, O. Ouari, J. Vasquez-Vivar, G. Cheng, M. Lopez and B. Kalyanaraman, *Chem. Rev*., 2017, **117**, 10043; (*g*) X. Zhang, J. Yin and J. Yoon, *Chem. Rev*., 2014, **114**, 4918; (*h*) X. Li, X. Gao, W. Shi and H. Ma, *Chem. Rev*., 2014, **114**, 590; (*i*) Y. Yang, Q. Zhao, W. Feng and F. Li, *Chem. Rev*., 2013, **113**, 192; (*j*) M. Vendrell, D. Zhai, J. C. Er and Y.-T. Chang, *Chem. Rev*., 2012, **112**, 4391; (*k*) L. Farzin, M. Shamsipur and S. Sheibani, *Talanta*, 2017, **174**, 619.
9 (*a*) M. Vedamalai and S. P. Wu, *Org. Biomol. Chem*., 2012, **10**, 5410; (*b*) L. Long, X. Tan, S. Luo and C. Shi, *New J. Chem*., 2017, **41**, 8899; (*c*) K. Kala, P. K. Vineetha and N. Manoj, *New J. Chem*., 2017, **41**, 5176; (*d*) J. Wang and X. Qian, *Org. Lett*., 2006, **8**, 3721.
10 (*a*) H. Jiang, J. Jiang, J. Cheng, W. Dou, X. Tang, L. Yang, W. Liu and D. Bai, *New J. Chem*., 2014, **38**, 109; (*b*) Y. Han, C. Yang, K. Wu, Y. Chen, B. Zhou and M. Xia, *RSC Adv*., 2015, **5**, 16723; (*c*) M. Santra, B. Roy and K. H. Ahn, *Org. Lett*., 2011, **13**, 3422; (*d*) W. Gong, B. Gao, J. Zhao and G. Ning, *J. Mater. Chem. A*, 2013, **1**, 5501; (*e*) X. Shang, N. Wang, R. Cerny, W. Niu and J. Guo, *ACS Sens*., 2017, **2**, 961.
11 (*a*) W. Xuan, C. Chen, Y. Cao, W. He, W. Jiang, K. Liu and W. Wang, *Chem. Commun*., 2012, **48**, 7292; (*b*) J. Liu, Y. Q. Sun, P. Wang, J. Zhang and W. Guo, *Analyst*, 2013, **138**, 2654; (*c*) J. Ding, H. Li, Y. Xie, Q. Peng, Q. Li and Z. Li, *Polym. Chem*., 2017, **8**, 2221; (*d*) J. Ding, H. Li, C. Wang, J. Yang, Y. Xie, Q. Peng, Q. Li and Z. Li, *ACS Appl. Mater. Interfaces*, 2015, **7**, 11369; (*e*) W. Shu, Y. Wang, L. Wu, Z. Wang, Q. Duan, Y. Gao, C. Liu, B. Zhu and L. Yan, *Ind. Eng. Chem. Res*., 2016, **55**, 8713; (*f*) Z. Zhang, B. Zhang, X. Qian, Z. Li, Z. Xu and Y. Yang, *Anal. Chem*., 2014, **86**, 11919; (*g*) A. S. Rao, D. Kim, T. Wang,

View Article Online
DOI: 10.1039/C7NJ03789A

K. H. Kim, S. Hwang and K. H. Ahn, *Org. Lett*., 2012, **14**, 2598; (*h*) W. Jiang and W. Wang, *Chem. Commun*., 2009, 3913.
12 (*a*) Y. Chen, C. Yang, Z. Yu, B. Chen and Y. Han, *RSC Adv*., 2015, **5**, 82531; (*b*) M. Tian and H. Ihmels, *Chem. Commun*., 2009, 3175; (*c*) N. Kumari, N. Dey, S. Jha and S. Bhattachary, *ACS Appl. Mater. Interfaces*, 2013, **5**, 2438; (*d*) M. Tian, L. Liu, Y. Li, R. Hu, T. Liu, H. Liu, S. Wang and Y. Li, *Chem. Commun*., 2014, **50**, 2055.
13 (*a*) B. Chen, J. Huang, H. Geng, L. Xuan, T. Xu, X. Li and Y. Han, *New J. Chem*., 2017, **41**, 1119; (*b*) L. Yang, X. Liu, L. Gao, F. Qi, H. Tian and X. Song, *RSC Adv*.,2015, **5**, 98154.
14 (*a*) J. A. Anshori, T. Slanina, E. Palao and P. Klán, *Photochem. Photobiol. Sci*., 2016, **15**, 250; (*b*) A. Rodriguez-Serrano, V. Rai-Constapel, M. C. Daza, M. Doerr and C. M. Marian, *Phys. Chem. Chem. Phys*., 2015, **17**, 11350.
15 Mercury Update: Impact of Fish Advisories. EPA Fact Sheet EPA-823-F-01-011; EPA, Office of Water: Washington, DC, 2001.

View Article Online
DOI: 10.1039/C7NJ03789A

A novel ESIPT-based fluorescent chemodosimeter for the detection of Hg^{2+} has been rationally designed and developed.